Array of Chemically Etched Fused-Silica Emitters for Improving the Sensitivity and Quantitation of Electrospray Ionization Mass Spectrometry

ARTICLE *in* ANALYTICAL CHEMISTRY · JULY 2007

Impact Factor: 5.64 · DOI: 10.1021/ac062417e · Source: PubMed

4 AUTHORS, INCLUDING:

Ryan Kelly
Pacific Northwest National Laboratory
61 PUBLICATIONS **1,603** CITATIONS
SEE PROFILE

Keqi Tang
Pacific Northwest National Laboratory
113 PUBLICATIONS **4,691** CITATIONS
SEE PROFILE

Richard D Smith
Pacific Northwest National Laboratory
1,132 PUBLICATIONS **46,141** CITATIONS
SEE PROFILE

Anal. Chem. **2007,** *79,* 4192−4198

Array of Chemically Etched Fused-Silica Emitters for Improving the Sensitivity and Quantitation of Electrospray Ionization Mass Spectrometry

Ryan T. Kelly, Jason S. Page, Keqi Tang, and Richard D. Smith*

Biological Sciences Division, Pacific Northwest National Laboratory, P.O. Box 999, Richland, Washington 99352

An array of emitters has been developed for increasing the sensitivity of electrospray ionization mass spectrometry (ESI-MS). The linear array consists of 19 chemically etched fused-silica capillaries arranged with 500 μm (center-to-center) spacing. The multiemitter device has a low dead volume to facilitate coupling to capillary liquid chromatography (LC) separations. The high aspect ratio of the emitters enables operation at flow rates as low as 20 nL/min/emitter, effectively extending the benefits of nanoelectrospray to higher flow rate analyses. To accommodate the larger ion current produced by the emitter array, a multicapillary inlet to the mass spectrometer was also constructed. The inlet, which matched the dimensions of the emitter array, preserved ion transmission efficiency. Standard reserpine solutions of varying concentration were electrosprayed at 1 μL/min using the multiemitter/multi-inlet combination, and the results were compared to those from a standard, single-emitter configuration. A 9-fold sensitivity enhancement was observed for the multiemitter relative to the single emitter. A bovine serum albumin tryptic digest was also analyzed, and a sensitivity increase ranging from 2.4- to 12.3-fold for the detected tryptic peptides resulted; the varying response was attributed to reduced ion suppression under the nanoESI conditions afforded by the emitter array. An equimolar mixture of leucine enkephalin and maltopentaose was studied to verify that ion suppression is indeed reduced for the multiplexed ESI (multi-ESI) array relative to a single emitter over a range of flow rates.

In the postgenomic era, proteomics has taken on an increasingly prevalent role for a variety of biological applications, from elucidating cell function[1−3] to identifying biomarkers as potential diagnostic tools.[4−6] Given the inherent complexity of biological samples, the development of technology to make broad, quantitative protein identifications in a reasonable period of time has been an enormous challenge. Capillary-based liquid chromatography (LC), combined with electrospray ionization mass spectrometry (ESI-MS), is an attractive platform[4,7,8] due to its suitability for automation and its high throughput relative to, for example, two-dimensional gel electrophoresis.[9,10] Although capillary LC/ESI-MS is presently capable of identifying thousands of proteins from a single experiment,[11] increased analytical sensitivity will be vital for further broadening protein coverage and reducing required sample sizes.

It is well-established that ESI-MS sensitivity increases as the liquid flow to the ESI emitter decreases.[12−14] This is mainly because the charged droplets formed during the electrospray process are smaller in the nanoESI regime (below ~100 nL/min) than at conventional flow rates.[12,15] Thus, solvent evaporates more efficiently for nanoESI, and fewer Coulombic fission events are required to create gas-phase ions.[12,15] Also, sampling efficiency is improved for nanoESI, as the enhanced desolvation allows the emitter to be positioned closer to the inlet of the mass spectrometer, further reducing ion losses.[16] Finally, because the electrospray current in cone−jet mode increases as the square root of the volumetric flow rate,[15] the number of available charges per analyte molecule increases as flow rate is reduced, enhancing ionization efficiency at low flow rates. The benefits of nanoESI for quantitation[17,18] are also in large part due to the smaller initial droplets; more efficient desolvation ensures

* Author to whom correspondence should be addressed. Phone: 509-376-0723. Fax: 509-376-7722. E-mail: rds@pnl.gov.

(1) Wollscheid, B.; Watts, J. D.; Aebersold, R. *Curr. Opin. Immunol.* **2004**, *16*, 337−344.
(2) Phillips, C. I.; Bogyo, M. *Cell. Microbiol.* **2005**, *7*, 1061−1076.
(3) Kussmann, M.; Affolter, M.; Fay, L. B. *Comb. Chem. High Throughput Screening* **2005**, *8*, 679−696.
(4) Qian, W.-J.; Jacobs, J. M.; Liu, T.; Camp, D. G.; Smith, R. D. *Mol. Cell. Proteomics* **2006**, *5*, 1727−1744.
(5) Bons, J. A. P.; Wodzig, W. K. W. H.; van Dieijen-Visser, M. P. *Clin. Chem. Lab. Med.* **2005**, *43*, 1281−1290.
(6) Omenn, G. S. *Proteomics* **2006**, *6*, 5662−5673.
(7) Shen, Y. F.; Smith, R. D. *Expert Rev. Proteomics* **2005**, *2*, 431−447.
(8) Swanson, S. K.; Washburn, M. P. *Drug Discovery Today* **2005**, *10*, 719−725.
(9) Ong, S.-E.; Pandey, A. *Biomol. Eng.* **2001**, *18*, 195−205.
(10) Wittmann-Liebold, B.; Graack, H.-R.; Pohl, T. *Proteomics* **2006**, *6*, 4688−4703.
(11) Shen, Y.; Zhang, R.; Moore, R. J.; Kim, J.; Metz, T. O.; Hixson, K. K.; Zhao, R.; Livesay, E. A.; Udseth, H. R.; Smith, R. D. *Anal. Chem.* **2005**, *77*, 3090−3100.
(12) Wilm, M. S.; Mann, M. *Int. J. Mass Spectrom. Ion Processes* **1994**, *136*, 167−180.
(13) Wahl, J. H.; Goodlett, D. R.; Udseth, H. R.; Smith, R. D. *Electrophoresis* **1993**, *14*, 448−457.
(14) Goodlett, D. R.; Wahl, J. H.; Udseth, H. R.; Smith, R. D. *J. Microcolumn Sep.* **1993**, *5*, 57−62.
(15) Fernandez de la Mora, J.; Loscertales, I. G. *J. Fluid Mech.* **1994**, *260*, 155−184.
(16) Smith, R. D.; Shen, Y.; Tang, K. *Acc. Chem. Res.* **2004**, *37*, 269−278.
(17) Schmidt, A.; Karas, M.; Dulcks, T. *J. Am. Soc. Mass Spectrom.* **2003**, *14*, 492−500.
(18) Valaskovic, G. A.; Utley, L.; Lee, M. S.; Wu, J.-T. *Rapid Commun. Mass Spectrom.* **2006**, *20*, 1087−1096.

10.1021/ac062417e CCC: $37.00
Published on Web 05/02/2007

that less "surface active" analytes are also ionized and better represented in the mass spectrum.[17] The increased amount of charge available per analyte molecule at reduced flow rates further minimizes suppression effects by reducing charge competition among different species.[19]

To realize the benefits of nanoESI for proteomics applications, we have previously used narrow-bore LC columns packed with very small particles to operate efficiently at low flow rates.[20,21] For example, 86 cm long, 15 μm i.d. capillaries packed with 3 μm particles provided a flow rate of ~20 nL/min when operated at 10 000 psi.[21] The sensitivity afforded by the nanoscale separation enabled more than 400 proteins to be identified from a 10 ng sample of *Deinococcus radiodurans* lysate tryptic digest. Unfortunately, there are several difficulties associated with operating LC separations at low-nanoliter/min flow rates, which have prevented their routine use for proteomics applications. First, packing particles into such narrow-bore capillaries is extremely difficult, requiring a great deal of skill and providing a low production yield.[16] Second, the low tolerance for dead volume precludes the use of conventional valving and sample loading. Instead, samples are loaded off-line onto a precolumn[22,23] in a process that would be difficult to automate. Finally, the sample loading capacity is very small, so care must be taken to avoid overloading the column. While such nanoscale separations continue to be valuable for applications in which available sample quantities are extremely limited, more conventional capillary LC separations (operated at ~1 μL/min) remain preferable for robust, automated analysis.

The simplest method to combine higher flow rate separations with nanoESI is to split the flow postcolumn such that most of the eluent is diverted to waste, leaving the desired flow rate for the MS analysis. Postcolumn splitting has been employed to reduce the flow rates delivered from normal-bore LC columns (0.2−1 mL/min) to improve ESI performance.[24−31] No efforts have been made to split the flow from capillary-based LC separations to, e.g., 20 nL/min for nanoESI. While postcolumn splitting allows better electrospray performance at the lower flow rate ESI operation, the inherent wastefulness of the process is evident: most of the sample is never analyzed.

A more attractive approach is to divide the flow from the LC column among multiple ESI emitters, and then efficiently transfer the increased ion current into the mass spectrometer. Compared with a split flow, multiplexed ESI (multi-ESI) should increase the MS signal in proportion to the number of emitters, assuming transfer efficiency is preserved. In addition to LC/MS, direct infusion experiments should also benefit from multi-ESI. For example, rather than infusing a sample at nanoESI flow rates and averaging for a long period of time to detect trace species, an array of emitters could be operated at a proportionately higher flow rate and achieve similar sensitivity in a fraction of the time, thus increasing throughput.

Multiplexed electrospray sources for fundamental studies that were operated at relatively high flow rates (i.e., several microliters/min/emitter) have been described.[32−37] To our knowledge, the only previous work to multiplex electrospray for increased ESI-MS sensitivity was performed in our laboratory.[38] A laser-machined polycarbonate microfluidic chip comprised of nine emitters was used to achieve stable multielectrosprays over a range of liquid flow rates, with a minimum flow rate per emitter of ~200 nL/min. By interfacing the emitter with a modified mass spectrometer inlet to accept the greater ion current, a 2−3-fold gain in sensitivity was achieved relative to that of a single emitter operated at the same flow rate.

Here we describe a linear array of 19 fused-silica emitters. In addition to more than doubling the number of emitters described in our previous work, there are several other key improvements. First, the high aspect ratio of the chemically etched emitters enables very low flow rate operation (~20 nL/min/emitter), where the benefits of nanoESI are most pronounced. Also, the dead volume of the device is similar to that of a single conventional pulled silica emitter, so the array should be readily coupled to LC separations. In direct infusion mode, the emitters demonstrated improved quantitation, and when used in combination with a modified mass spectrometer inlet, they produced an ~9-fold gain in sensitivity compared with that of a single-emitter/single-inlet setup.

EXPERIMENTAL SECTION

Sample Preparation. Water was purified using a Barnstead Nanopure Infinity system (Dubuque, IA). Methanol (MeOH; HPLC grade) and 49% hydrofluoric acid were from Fisher Scientific (Fair Lawn, NJ). Reserpine, ammonium acetate, acetic acid (HAc), leucine enkephalin, maltopentaose, and bovine serum albumin (BSA) were purchased from Sigma-Aldrich (St. Louis, MO). BSA was digested with trypsin as described previously[39] and diluted to 0.1 mg/mL in ammonium bicarbonate.

(19) Tang, K.; Page, J. S.; Smith, R. D. *J. Am. Soc. Mass Spectrom.* **2004**, *15*, 1416−1423.
(20) Shen, Y.; Moore, R. J.; Zhao, R.; Blonder, J.; Auberry, D. L.; Masselon, C.; Paša-Tolić, L.; Hixson, K. K.; Auberry, K. J.; Smith, R. D. *Anal. Chem.* **2003**, *75*, 3596−3605.
(21) Shen, Y.; Tolić, N.; Masselon, C.; Paša-Tolić, L.; Camp, D. G. I.; Hixson, K. K.; Zhao, R.; Anderson, G. A.; Smith, R. D. *Anal. Chem.* **2004**, *76*, 144−154.
(22) Shen, Y.; Tolić, N.; Masselon, C.; Paša-Tolić, L.; Camp, D. G.; Lipton, M. S.; Anderson, G. A.; Smith, R. D. *Anal. Bioanal. Chem.* **2004**, *378*, 1037−1045.
(23) Luo, Q.; Tang, K.; Yang, F.; Elias, A.; Shen, Y.; Moore, R. J.; Zhao, R.; Hixson, K. K.; Rossie, S. S.; Smith, R. D. *J. Proteome Res.* **2006**, *5*, 1091−1097.
(24) Tyrefors, N.; Hyllbrant, B.; Ekman, L.; Johansson, M.; Langstrom, B. *J. Chromatogr., A* **1996**, *729*, 279−285.
(25) Tracqui, A.; Kintz, P.; Ludes, B.; Mangin, P. *J. Chromatogr., B* **1997**, *692*, 101−109.
(26) Taylor, P. J.; Jones, C. E.; Dodds, H. M.; Hogan, N. S.; Johnson, A. G. *Ther. Drug Monit.* **1998**, *20*, 691−696.
(27) Fuh, M.-R.; Hsieh, C.-J. *J. Chromatogr., B* **1999**, *736*, 167−173.
(28) Rajanikanth, M.; Madhusudanan, K. P.; Gupta, R. C. *Biomed. Chromatogr.* **2003**, *17*, 440−446.
(29) Gangl, E. T.; Annan, M.; Spooner, N.; Vouros, P. *Anal. Chem.* **2001**, *73*, 5635−5644.
(30) Andrews, C. L.; Yu, C.-P.; Yang, E.; Vouros, P. *J. Chromatogr., A* **2004**, *1053*, 151−159.
(31) Andrews, C. L.; Li, F.; Yang, E.; Yu, C.-P.; Vouros, P. *J. Mass Spectrom.* **2006**, *41*, 43−49.
(32) Rulison, A. J.; Flagan, R. C. *Rev. Sci. Instrum.* **1993**, *64*, 683−686.
(33) Almekinders, J. C.; Jones, C. *J. Aerosol Sci.* **1999**, *30*, 969−971.
(34) Regele, J. D.; Papac, M. J.; Rickard, M. J. A.; Dunn-Rankin, D. *J. Aerosol Sci.* **2002**, *33*, 1471−1479.
(35) Bocanegra, R.; Galan, D.; Marquez, M.; Loscertales, I. G.; Barrero, A. *J. Aerosol Sci.* **2005**, *36*, 1387−1399.
(36) Duby, M.-N.; Deng, W.; Kim, K.; Gomez, T.; Gomez, A. *J. Aerosol Sci.* **2006**, *37*, 306−322.
(37) Deng, W.; Klemic, J. F.; Li, X.; Reed, M. A.; Gomez, A. *J. Aerosol Sci.* **2006**, *37*, 696−714.
(38) Tang, K.; Lin, Y.; Matson, D. W.; Kim, T.; Smith, R. D. *Anal. Chem.* **2001**, *73*, 1658−1663.

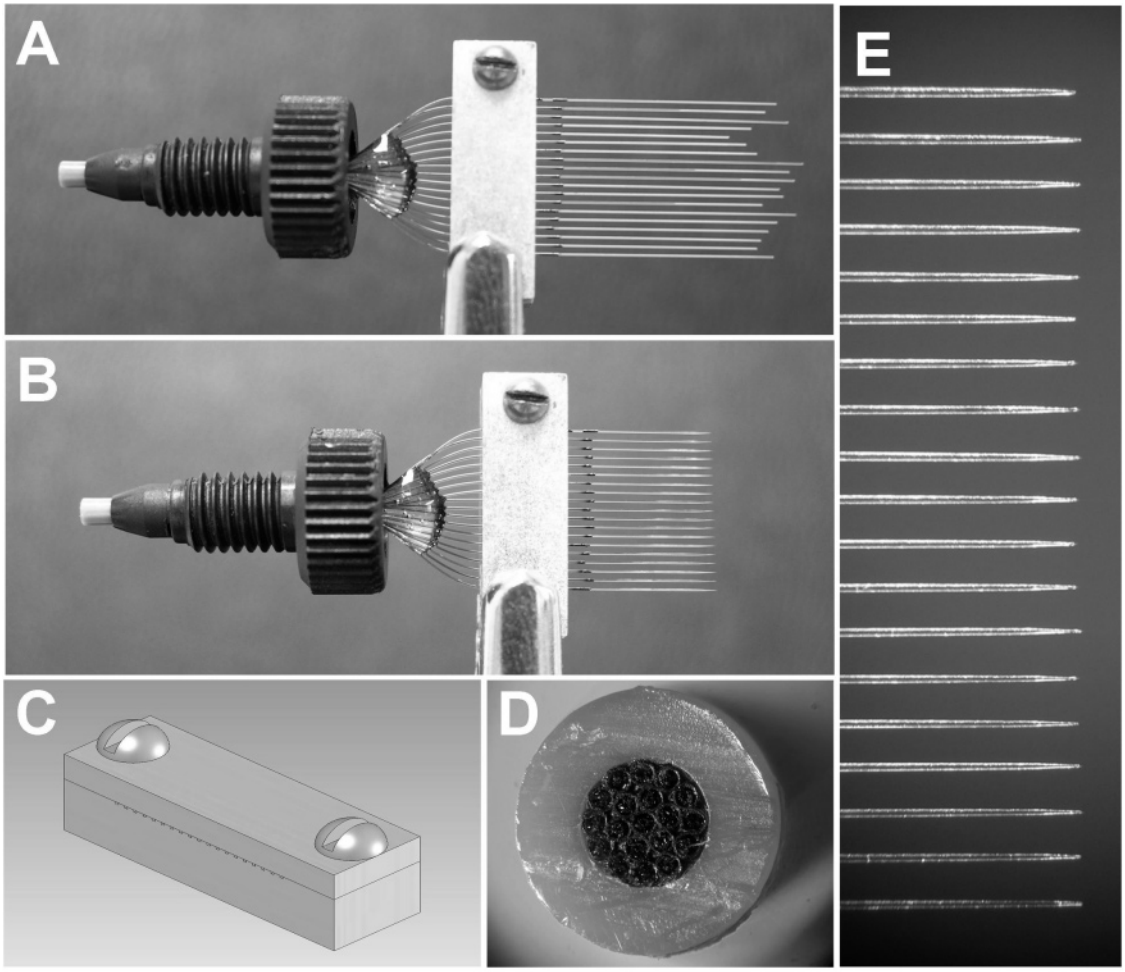

Figure 1. Device images: (A) array of 19 emitters before etching the capillaries in HF; (B) completed device; (C) drawing of the aluminum holder used for capillary alignment; (D) photomicrograph of the emitter inlet with the capillaries inside the PEEK tubing sleeve; (E) close-up view of the etched emitter array.

The solution was then further diluted to 25 μg/mL in 1:1 MeOH/H_2O + 1% HAc.

Fabrication of Emitter Arrays. To create the emitter arrays (Figure 1), a section of fused-silica tubing (19 μm i.d., 150 μm o.d.; Polymicro Technologies, Phoenix, AZ) was cut into 19 capillaries that were each ~6 cm long. The end ~1 cm of polyimide was burned and then removed from each capillary with a MeOH-soaked cloth. An aluminum holder was created to enable the capillaries to be aligned in parallel and spaced evenly (500 μm center-to-center spacing; see Figure 1A–C). The capillaries were threaded through the holes created by the grooved base and the cover (Figure 1C) such that the capillary ends protruded 1–2 cm (Figure 1A). The screws on the holder were then tightened to lock the capillaries in place, and the capillary ends that were still protected by polyimide were bundled together and fed through an ~1.5 cm long PEEK tubing sleeve (750 μm i.d., $^1/_{16}$ in. o.d.; Upchurch Scientific, Oak Harbor, WA). Epoxy (no. 14250, Devcon, Danvers, MA) was used to fill the tubing sleeve around the capillaries. The epoxy was fully cured by heating the devices at 70 °C for 4 h. No peaks associated with the epoxy were observed in the mass spectra. The device inlet (Figure 1D) was created by cutting excess capillary and tubing with a razor blade or with a rotary tubing cutter (TC-10, Scientific Systems, State College, PA). A nut and ferrule (F-195x, Upchurch Scientific) were placed on the tubing sleeve, enabling connection to a stainless steel union (Upchurch Scientific). The capillary ends were then etched using a method that was described previously for creating individual silica emitters.[40] Briefly, water was pumped through the array of capillaries at a rate of 1.9 μL/min (0.1 μL/min/capillary) and the capillary ends were immersed in 49% hydrofluoric acid. The capillaries were left to etch until all silica touching the HF bath had been completely removed, leaving high aspect ratio, externally tapered emitters of uniform length (Figure 1, parts B and E). The single emitters used for comparison were created as described previously.[40]

MS Instrumentation. An Agilent MSD1100 (Santa Clara, CA) single-quadrupole mass spectrometer equipped with an in-house-built ESI/ion funnel source was used; the ion funnel is similar to what was described previously.[41] To accommodate the increased conductance of the multicapillary interface described below, an

(39) Tang, K.; Li, F.; Shvartsburg, A. A.; Strittmatter, E. F.; Smith, R. D. *Anal. Chem.* **2005**, *77*, 6381–6388.

(40) Kelly, R. T.; Page, J. S.; Luo, Q.; Moore, R. J.; Orton, D. J.; Tang, K.; Smith, R. D. *Anal. Chem.* **2006**, *78*, 7796–7801.

(41) Shaffer, S. A.; Tolmachev, A.; Prior, D. C.; Anderson, G. A.; Udseth, H. R.; Smith, R. D. *Anal. Chem.* **1999**, *71*, 2957–2964.

additional "high-pressure" ion funnel, operated at 16 torr,[42] was incorporated in front of the standard ion funnel, which operated at 2 torr. The 16 torr ion funnel chamber was pumped by a 20.4 m^3/h (E1M18, BOC Edwards, Wilmington, MA) and a 19.8 m^3/h (D16A, Leybold, Cologne, Germany) rough pump. The 2 torr ion funnel chamber was pumped by an E1M18 rough pump that also backed the turbomolecular pumps on the mass spectrometer. The ion funnels were made by stacking 100 ring electrodes made from 0.5 mm thick brass plates that were separated by 0.5 mm thick Teflon spacers. The front section of the ion funnel consisted of 58 electrodes having a constant i.d. of 25.4 mm. The tapered ion funnel section was made from 42 electrodes that decreased linearly in i.d. from 25.4 to 2.5 mm. These electrodes were followed by a dc-only electrode (conductance limit) with an i.d. of 2.0 mm. A 6.5 mm diameter "jet disrupter" electrode[43] was located ~2 cm from the entrance of the ion funnel (at plate 20 of the 100 plate stack). The electrical circuitry for each ion funnel was mounted onto two circuit boards that consisted of a chain of 500 kΩ resistors for the dc gradient and 10 nF capacitors for the rf voltage. The boards were attached to the ion funnels with two custom zero insertion force connectors (Tactic Electronics, Plano, TX). An rf of 1.2 MHz at 190 V_{p-p} (peak-to-peak) and 730 kHz at 100 V_{p-p} was applied to the 16 and 2 torr ion funnels, respectively, by custom high-Q heads and rf power amplifiers. The dc voltages were supplied by a nine-output dc power supply (model TD-9500, Spectrum Solutions, Russellton, PA). A dc gradient of ~19 V/cm was applied to each ion funnel: 400 and 210 V were applied to the first and last plates of the 16 torr ion funnel and 200 and 10 V were applied to the first and last plates of the 2 torr ion funnel. The conductance limit electrode for each ion funnel was biased at 5 V less than the last rf/dc electrode, and the jet disrupter voltage was adjusted for maximum ion transmission, approximately 15−25 V less than the first funnel electrode voltage. High voltage was applied to the ESI emitter via a Bertan power supply (model 205B-03R, Hicksville, NY).

A multicapillary inlet was created to enable each individual emitter from the multiemitter array to line up with a heated capillary inlet. The inlet was made by aligning 19 stainless steel capillaries, 400 μm i.d./500 μm o.d. (part no. 89935K236, McMaster-Carr, Los Angeles, CA), side-by-side and soldering them in a stainless steel heating block containing a brass insert to hold the capillaries in a straight line. The brass insert also served as a heat conductor. After soldering, the ends of the heating block were machined down to a length of 6.4 cm. The multicapillary inlet was heated by two 100 W cartridge heaters (Watlow, St. Louis, MO), and the temperature was regulated by a temperature controller (model CN9000A, Omega, Stanford, CT). The heated capillary inlet was biased to a potential 10 V higher than the dc potential on the first ion funnel electrode.

Experiments to quantify ion suppression were performed using an unmodified Finnigan LCQ mass spectrometer (San Jose, CA). For the LCQ experiments, an ESI potential of 1.6 kV was used for both single emitters and multiemitters, the gap between the emitters and the inlet was 1.5 mm, and the temperature of the MS inlet capillary was 170 °C.

(42) Ibrahim, Y.; Tang, K.; Tolmachev, A. V.; Shvartsburg, A. A.; Smith, R. D. *J. Am. Soc. Mass Spectrom.* **2006**, *17*, 1299−1305.
(43) Kim, T.; Tang, K.; Udseth, H. R.; Smith, R. D. *Anal. Chem.* **2001**, *73*, 4162−4170.

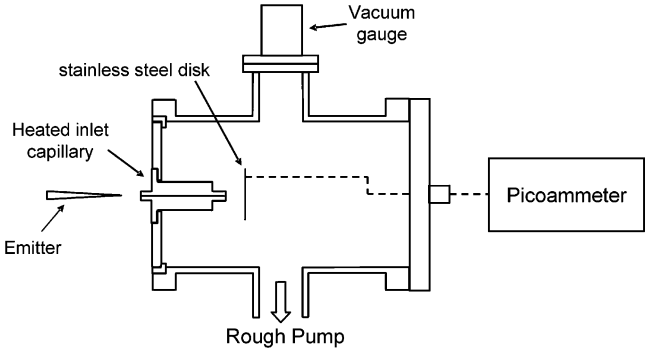

Figure 2. Schematic of the benchtop ESI interface used to simulate the first (rough-pumped) stage of the mass spectrometer. The multicapillary inlet and the single-capillary inlet (shown) were interchangeable.

ESI Current Measurements. Measurements of ESI currents transmitted through the heated capillary inlets were made using a separate ESI source and interface that was constructed from a four-way reducing cross with a 6 in. main flange, as shown in Figure 2. An E1M18 rough pump was used to pump the chamber, and a strain gauge (BOC Edwards) measured the pressure. The front flange served as a holder for the ESI inlet, and the back flange contained a BNC electrical feedthrough. The inlets were heated and the temperature was regulated as for the mass spectrometer inlet described above. To detect the current transmitted through the inlet, a 4 cm diameter stainless steel disk was positioned 1 cm from the exit of the inlet. This disk was connected to the BNC electrical feedthrough, creating a charge collector. The ESI current was obtained by averaging 100 consecutive measurements using a picoammeter with built-in data acquisition capabilities (model No. 6485, Keithley, Cleveland, OH).

SAFETY INFORMATION

HF is extremely hazardous and corrosive. Extreme care must be taken to prevent exposure to HF liquid or vapor. HF solutions should be used in a ventilated hood, and appropriate protective equipment should be worn.

RESULTS AND DISCUSSION

The recently developed[40] ability to chemically etch the capillaries comprising the multiemitters such that they protruded evenly (Figure 1E) was crucial to the success of this approach, as small variations in length or spacing would lead to nonuniform performance for the emitters comprising the array. To achieve uniform lengths, the capillaries needed to be positioned a small distance from each other so that each formed its own meniscus in the HF solution and etched independently of the others. This was accomplished using an aluminum holder (Figure 1C), which held the emitters parallel and evenly spaced. To increase emitter density using this approach much beyond the present embodiment, capillaries having smaller outer diameters could be used. Figure 1, parts A and B, shows photographs of an emitter array before and after etching, respectively, which illustrate that alignment during assembly is unnecessary; excess silica is removed from all emitters during the etching process. Manual alignment of pulled silica emitters with such precision would be very difficult.

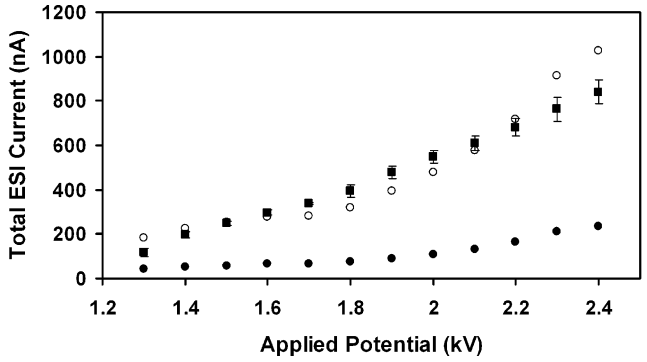

Figure 3. Total electrospray currents from a single emitter (●) and the multiemitter array (■) vs applied potential. The additional data series (○) shows the current from the single emitter multiplied by $19^{1/2}$ for comparison with theory. Error bars for the single emitter were too small to display. The solution was 1:1 H_2O/MeOH + 1% HAc, the distance from the emitter to the ground plate was 1.5 mm, and the total flow rate was 1.0 μL/min.

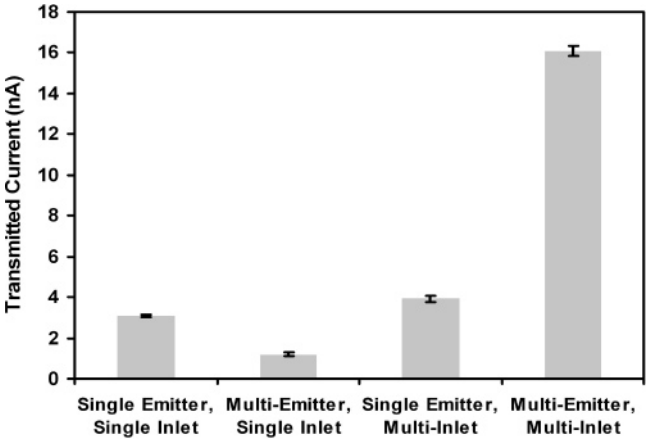

Figure 4. Currents transmitted to a charge collector in a chamber simulating the rough vacuum stage of a mass spectrometer. In all cases, the applied ESI potential was 1350 V, the distance from the emitter(s) to the inlet(s) was 1.0 mm, the temperature of the inlets was 120 °C, the flow rate was 1.0 μL/min, and the solvent was 1:1 H_2O/MeOH + 1% HAc.

Additionally, the chemical etching procedure provides emitters that do not taper internally, virtually eliminating clogging from particulates and extending emitter lifetime.[40] Another significant feature of the devices is their low dead volume, which is limited to the internal volume of the capillaries themselves. For example, a 4 cm long, 75 μm i.d. pulled emitter[44] has an internal volume of ~180 nL, very similar to the ~200 nL volume of the 19-emitter arrays presented here. The emitter dead volume could be further reduced by using narrower bore capillaries or filling with polymer monolith.[44] The low dead volume of the emitter arrays, combined with their ready coupling to capillary columns via standard stainless steel unions, should make their implementation with LC/MS straightforward.

To assess the performance of the multi-ESI arrays, ion current measurements were made over a broad range of voltages, which were then compared with the ion currents of a single emitter operating under the same conditions, as shown in Figure 3. Also shown in Figure 3 is the current from the single emitter at each ESI voltage multiplied by $19^{1/2}$ (open circles). Tang, et al.[38] have shown that in a stable cone−jet mode, the total electrospray current should scale as the square root of the number of emitters, provided that the total flow rate is held constant. The scaled single-emitter voltages in Figure 3 therefore provide theoretical currents for the multiemitter array, assuming each emitter operates independently. We observe that close agreement between measured and theoretical currents for the multiemitter holds over a broad range of voltages, as long as the internal resistance of the emitter array and the individual emitters is matched. To match internal resistance, the single emitter had an i.d. of 77 μm and a length of ~3.2 cm. Interestingly, the increase in current for the multiemitter is more linear than for the individual emitter; i.e., there is no plateau in current observed for cone−jet mode as with the single emitter (between 1.5 and 1.8 kV). This is likely due to the individual emitters entering stable cone−jet mode at slightly different voltages, which smoothes out the current profile. A potential concern with multi-ESI devices is electric field inhomogeneity among the emitters due to cross-talk or shielding effects.[32,34,37] Because the currents observed with the multiemitter array agreed closely with the expected currents, and because the minimum voltage required to achieve stable electrospray across all the emitters in the array was generally only slightly (~100 V) higher than for a single emitter, we conclude that electric field shielding does not greatly impact the performance of the present design.

The increased ion currents generated by the multi-ESI arrays are of little benefit if the additional current cannot be efficiently delivered into the mass spectrometer. We therefore concurrently developed a modified mass spectrometer inlet. For this work, the modified inlet consisted of a linear array of 19 (400 μm i.d.) stainless steel capillaries as described in the Experimental Section. Ion transmission efficiency was evaluated by measuring the ion currents that passed through the individual and multi-inlets to a charge collector in a vacuum chamber that was used to model the first inlet (rough-pumped) stage of the mass spectrometer (Figure 2). The distance of the emitters to the inlet, the pressure inside the vacuum chamber, and the temperature of the heated capillary inlets were set to match conditions used for MS analyses (see below). Figure 4 compares ion currents transmitted from a single emitter and a multiemitter through the single-capillary and multicapillary inlets. When using the standard configuration of a single emitter coupled to a single-capillary inlet, the transmitted current was ~3.1 nA. By employing the multiemitter and the multicapillary inlet, a greater than 5-fold increase in transmitted current was observed, and by taking the ratio of transmitted current to total ESI current in each case, we found that the transmission efficiency improved slightly, from 4.9% to 6.2%. Also shown in Figure 4 are the transmitted currents when a single emitter was used with the multicapillary inlet and when a multiemitter was interfaced with a single-capillary inlet. The multicapillary inlet slightly improved transmission efficiency for the individual emitter, and transmission was greatly reduced when the multi-ESI source was coupled with the single-capillary inlet, as most of the emitters were too far off axis to be sampled. While the increase in current transmission is notable, there may be other heated capillary inlet arrangements that prove much more ef-

(44) Koerner, T.; Turck, K.; Brown, L.; Oleschuk, R. D. *Anal. Chem.* **2004**, *76*, 6456−6460.

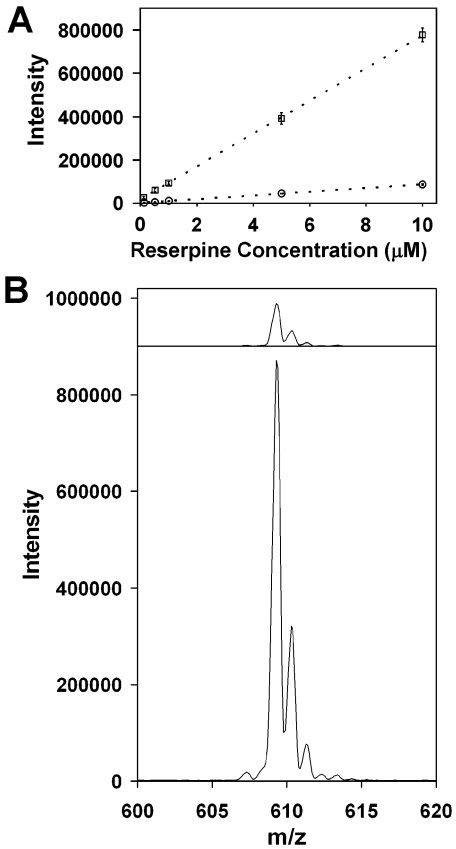

Figure 5. (A) MS intensity vs reserpine concentration using (○) a single-emitter/single-inlet configuration and (□) a multiemitter coupled to a multicapillary inlet. (B) Mass spectra for 10 μM reserpine using a single emitter (top) and a multiemitter (bottom). The emitter−inlet distance was 1.0 mm, and the solvent was 1:1 H_2O/MeOH + 1% HAc.

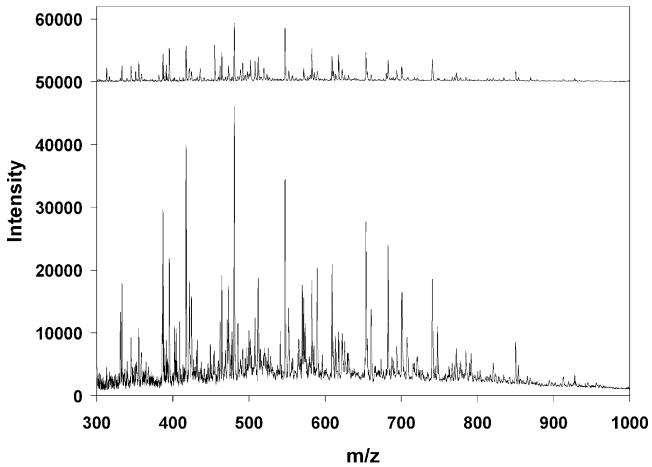

Figure 6. Mass spectra for 25 μg/mL BSA using a single emitter (top) and a multiemitter (bottom).

ficient. We continue to explore alternative inlet configurations to enhance ion transmission efficiency for multi-ESI sources.

To verify that the increased transmitted ion current translated to enhanced sensitivity in the mass spectrometer, we analyzed solutions of reserpine at various concentrations using both standard and multiemitter/multicapillary inlet configurations (Figure 5A). With the multiemitter combined with the multicapillary inlet, the sensitivity was increased by a factor of ~9. With both arrangements, the response of the mass spectrometer to concentration was linear, so the signal enhancement was preserved throughout the entire concentration range tested (100 nM to 10 μM). Figure 5B shows mass spectra of 10 μM reserpine for the two configurations on the same intensity scale for comparison. An ~9-fold sensitivity gain is greater than the increase in transmitted current (Figure 4), indicating that the "quality" of the delivered current also improves. This is attributed to enhanced desolvation resulting from the much smaller charged droplets generated by the nanoelectrosprays in the case of multiemitters. More of the current that enters the mass spectrometer is composed of individual ions that can be detected, rather than charged droplets that cannot.

Table 1. Sensitivity Enhancement for BSA Peptides from the Mass Spectra in Figure 6[a]

peptide	m/z	enhancement factor
GLVLIAFSQYLQQCPFDEHVK; 3+	812.8	5.0
DAFLGSFLYEYSR	784.4	9.9
LGEYGFQNALIVR	740.4	5.2
YICDNQDTISSK	693.8	4.4
RHPYFYAPELLYYANK; 3+	682.7	7.0
LKPDPNTLCDEFKADEK; 3+	655.3	5.5
QEPERNECFLSHKDDSPDLPK; 4+	622.0	5.0
LFTFHADICTLPDTEK; 3+	618.0	2.4
ECCDKPLLEK	589.3	12.3
LVNELTEFAK	582.3	3.5
DDPHACYSTVFDKLK; 3+	580.3	4.9
KQTALVELLK	571.9	7.4
CCTESLVNR	512.7	4.4
RHPEYAVSVLLR; 3+	480.6	4.9
LKECCDKPLLEK; 3+	473.5	6.7
AEFVEVTK	461.8	4.8
LSQKFPK	424.3	9.8
LVTDLTK	395.2	4.1
AWSVAR	345.2	3.7
KFWGK	333.2	7.1

[a] Peptides were doubly charged except as noted.

The data from Figure 5A were also used to compare the ESI stability between the multiemitter and single-emitter platforms by calculating the relative standard deviation (RSD) of the total ion signal for the measurements, which were each an average of 10 scans. Each data point in Figure 5A is based on 3 replicates, providing 15 measurements for each platform. The average RSD was 3.3% and 4.6% for the multiemitter and individual emitter, respectively. This shows that the two platforms have comparable stability, and the slight improvement for the multiemitter may indicate that the fluctuations from the individual emitters comprising the array offset each other to improve the stability of the measured signal.

We also tested the multiemitter/multicapillary inlet performance using a complex peptide mixture (an albumin tryptic digest) and found a large sensitivity gain relative to that of the single-emitter/single-inlet as well. Figure 6 compares the results between the individual and multiplexed emitter configurations. Table 1 shows the average gain in peak heights for the species that were compared. While the multiemitter consistently delivered increased sensitivity, the gains ranged widely among different species, from 2.4−12.3-fold, suggesting differences in ionization

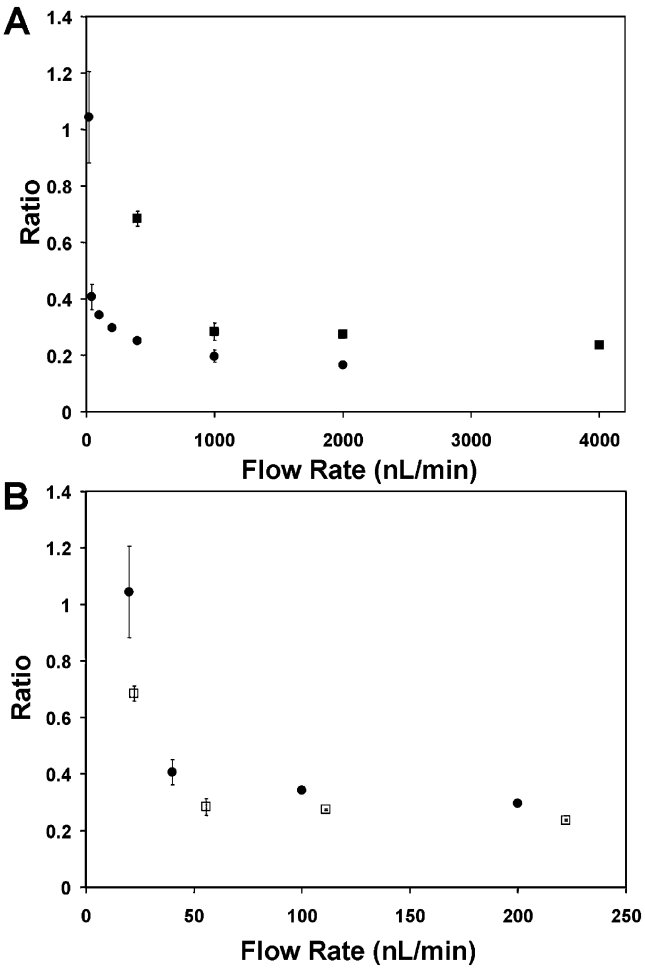

Figure 7. (A) Ratio of maltopentaose/leucine enkephalin intensities vs total flow rate for (●) an individual emitter and (■) an emitter array. (B) Ratio of maltopentaose/leucine enkephalin intensities vs flow rate, in terms of the average flow rate per capillary, shown for the individual emitter (●) and the multiemitter (□) arrangements. The solution consisted of leucine enkephalin and maltopentaose (10 μM each) in 1:1 10 mM aqueous ammonium acetate/MeOH.

efficiencies for the two analyses. Because the benefits of reduced flow rate ESI for minimizing ion suppression are well-established,[17,18,29,45] it is reasonable to assume that peak intensities from the multiemitter analysis better reflect the concentrations of the species in solution.

To quantitatively assess the reduction in ion suppression, we analyzed an equimolar mixture of the peptide leucine enkephalin and the oligosaccharide maltopentaose, using conditions adapted from Schmidt et al.[17] As the flow rate is reduced, the ratio of intensity of the maltopentaose (which is typically highly suppressed) to leucine enkephalin increases. For a single emitter, the increase in maltopentaose/leucine enkephalin is most dramatic below ~100 nL/min, and an equimolar response is observed at 20 nL/min (Figure 7A). We compared the intensity ratios versus flow rate with those observed using the multiemitter. Figure 7A shows the ratios of peak intensities versus total flow rate for the multiemitter and a 20 μm i.d. single emitter. A narrow-bore single emitter allowed flow rates as low as 20 nL/min to be achieved. At each of the flow rates where the two devices overlapped, quantitation (i.e., more equivalent ionization efficiencies) was improved when the multi emitter was used, as indicated by a larger ratio of maltopentaose/leucine enkephalin. The greatest performance gap between the two emitters was evident at 0.4 μL/min, where each of the multiemitter capillaries was operating at close to 20 nL/min. Figure 7B shows the ratios obtained using the single emitter at flow rates between 20 and 200 nL/min, as well as the ratios from the multiemitter, in which the total flow rate was divided by 19 to indicate the average flow rate per emitter. The intensity ratios versus normalized flow rate nearly coincide with those of the single emitter.

CONCLUSIONS

We have demonstrated an array of 19 high aspect ratio chemically etched fused-silica emitters for extending the benefits of nanoESI to higher flow rate analyses. At 1 μL/min, an ~9-fold sensitivity enhancement relative to that of a single emitter was achieved for reserpine over a broad range of concentrations. To realize the improved sensitivity, the multiemitter was interfaced with a modified MS inlet that effectively preserved ion transfer efficiency. Enhanced quantitation was also demonstrated by measuring the ratio of intensity of two standard analytes at different flow rates for the array of 19 emitters and comparing the result with an individual emitter. Future work will focus on improvements to the modified mass spectrometer inlet, which could substantially increase ion transfer efficiency. Also, the emitter arrays will be interfaced with LC separations analyzing proteomic samples for further characterization and evaluated for potentially improved quantitation, e.g., for "label-free" proteomics applications.[23,46–48]

ACKNOWLEDGMENT

We thank Heather Mottaz for preparing the BSA digest sample and Dr. Fumin Li for assistance in identifying the BSA peptides. Portions of this research were supported by the U.S. Department of Energy (DOE) Office of Biological and Environmental Research, the NIH National Center for Research Resources (RR018522), and the NIH National Cancer Institute (R21 CA126191). Experimental portions of this research were performed in the Environmental Molecular Sciences Laboratory, a U.S. DOE national scientific user facility located at the Pacific Northwest National Laboratory (PNNL) in Richland, Washington. PNNL is a multiprogram national laboratory operated by Battelle for the DOE under Contract No. DE-AC05-76RLO 1830.

Received for review December 21, 2006. Accepted March 22, 2007.

AC062417E

(45) Bahr, U.; Pfenninger, A.; Karas, M.; Stahl, B. *Anal. Chem.* **1997**, *69*, 4530–4535.
(46) Ono, M.; Shitashige, M.; Honda, K.; Isobe, T.; Kuwabara, H.; Matsuzuki, H.; Hirohashi, S.; Yamada, T. *Mol. Cell. Proteomics* **2006**, *5*, 1338–1347.
(47) Le Bihan, T.; Goh, T.; Stewart, I. I.; Salter, A. M.; Bukhman, Y. V.; Dharsee, M.; Ewing, R.; Wisniewski, J. R. *J. Proteome Res.* **2006**, *5*, 2701–2710.
(48) Zhang, B.; VerBerkmoes, N. C.; Langston, M. A.; Uberbacher, E.; Hettich, R. L.; Samatova, N. F. *J. Proteome Res.* **2006**, *5*, 2909–2918.